



Brønsted acidic SILP-based catalysts with $H_3PMo_{12}O_{40}$ or $H_3PW_{12}O_{40}$ in the oxidative desulfurization of fuels

A.A. Bryzhin^a, M.G. Gantman^b, A.K. Buryak^c, I.G. Tarkhanova^{a,*}

^a M.V. Lomonosov Moscow State University, Moscow, Russia

^b Friedrich-Alexander Universität Erlangen-Nürnberg, FAU, Erlangen, Germany

^c Frumkin Institute of Physical Chemistry and Electrochemistry, Russian Academy of Sciences, Moscow, Russia



ARTICLE INFO

Keywords:

Catalytic oxidative desulfurization
Hydrogen peroxide
Phosphomolybdc and phosphotungstic
heteropolyacids
Supported ionic liquid phase

ABSTRACT

In this manuscript novel heterogeneous catalysts for fuel desulfurization via peroxide oxidation are reported. The obtained catalysts combine high catalytic activity and stability with perfect synthetic availability, their composition and structure were ascertained. The catalysts represent supported ionic liquid phases (SILPs): Brønsted acidic ILs, namely 4-(3'-ethylimidazolium)-butanesulfonate, with two heteropolyacids (HPA) (sulfated ionic liquid protonated by $H_3PMo_{12}O_{40}$ or $H_3PW_{12}O_{40}$). Silica and γ -Al₂O₃ were used as support materials. These compositions ensure higher stability of heteropolyanions and make the catalyst stable over several successive oxidation cycles. The most active catalyst based on phosphomolybdc acid provides a high conversion rate for thiophene, thioanisole, and dibenzothiophene (turn over frequency of about 150–1200 h⁻¹ per mole of HPA). Another important benefit of the reported systems is the desulfurization of diesel fuel with a very high efficiency (residual amount of sulfur < 10 ppm) under mild conditions.

1. Introduction

In recent years, removal of sulfur compounds from oil feedstock has become a pressing problem due to the existing regulations directed to protection of the environment. Sulfur compounds deactivate some oil refining catalysts, cause corrosion of equipment, promote the formation of acid rains, and affect human health and environment. For preventing this adverse influence, a variety of approaches are considered, directed towards the production of fuels with ultralow sulfur contents (< 10 ppm) [1].

The traditional hydrodesulfurization process is widely used to reduce the sulfur content in the hydrocarbon feedstock. This process is efficient for the removal of thiols and disulfides and is less efficient in relation to heterocyclic sulfur compounds, for example, dibenzothiophene derivatives [2,3]. Therefore, complete removal of sulfur compounds from hydrocarbon feedstock requires conducting the process at high pressure and temperature, which markedly increases the cost of oil refining [4]. Due to these limitations, an important challenge is the search for alternative methods for processing oil feedstock that would support the existing traditional processes.

Apart from hydrodesulfurization, hydrogen-free methods are also employed to remove sulfur compounds, such as biodesulfurization [5,6], adsorption [7,8], extraction [9–11], and oxidative

desulfurization (ODS) [12,13]. Oxidative desulfurization is the most promising among these methods, due to its efficiency and mild reaction conditions [14]. The process can be conducted using the conventional oil refining equipment in combination with the industrial hydrodesulfurization process. The oxidative desulfurization leads to increasing polarity and molecular mass of sulfur compounds, which facilitates their removal by extraction or adsorption [14,15]. An oxidant is the key component of the process. The possible oxidants are hydrogen peroxide [16,17], organic peroxides [18,19], oxygen [20,21], and ozone [22]. In particular, cyclohexanone peroxide is effective organic oxidizing agent allowing to quickly carry out ODS with minimal oxidant consumption [23–25]. Hydrogen peroxide is used most widely, since it is highly reactive, environmentally friendly, and readily available [26]. Currently, single and mixed oxides and salts of transition metals in high oxidation states are used as ODS catalysts [27–32]. Particular attention is attracted to ionic liquids containing the above-mentioned compounds in the anionic or cationic moiety [33]. With targeted selection of components of cation–anion pairs [34], ionic liquids can be applied as extractants [35,36] or homogeneous catalysts [37,38] in the desulfurization process. However, the key problem hampering the industrial use of many ILs is their cost [33]. Methods for the recovery and reuse of ionic liquids are known [39], but for decreasing the consumption of ILs and for simplifying the procedure of

* Corresponding author.

E-mail address: itar_msu@mail.ru (I.G. Tarkhanova).

catalyst separation from the reaction products, ILs are immobilized on a support surface [40,41]. In our study, systems obtained by physical adsorption of ILs on the surface of mineral supports were used for the oxidation of typical representatives of organosulfur oil components (thiophene, dibenzothiophene, thioanisole). Most of the studies aimed at decreasing the sulfur content in the hydrocarbon feedstock are concentrated on the removal of thiophene derivatives. However, it is known that thiophene is the most difficult to oxidize, because of low electron density of sulfur [42,43]. Therefore, our main goal was to develop compositions that would be stable and catalytically active towards sulfur compounds of crude oil, first of all, thiophene. As the active component of the catalyst, we used sulfated IL, 4-(3'-ethylimidazolium)-butanesulfonate, protonated by Mo- and W-based heteropolyacids. Ionic liquids of this class have proved themselves as active extractants and catalysts [44–46] for thiophene derivatives; however, the use of supported ionic liquid phases (SILP), based on these ILs is till present not described. The only drawback of the ODS is that in most cases sulfurcontaining compounds are oxidized to sulfoxides or sulfones, which can be easily separated from oil, but still have to be converted into valuable products. On that reason the catalyst, which would enable direct oxidation of sulfur containing compounds into sulfuric acids are of particular interest. This is the second reason, why namely Brønsted acidic ILs, protonated with heteropolyacids (HPAs) were chosen as the catalysts.

We have used dibenzothiophene, thiophene and thioanisole as model substrates. Dibenzothiophene and thioanisole are typical representatives of sulfides and sulfur-containing heterocycles of diesel, and DBT is the most inactive in hydrodesulfurization, but can be removed by oxidation [1,47,48]. Thiophene is of interest for two reasons. First, it is the most difficult to oxidize among sulfur-heterocycles [1]. Secondly, it can oxidize to form different products [49–51]. We have got catalysts oxidizing thiophene to sulfuric acid.

In order to increase the efficiency of oxidant consumption, we decided to use an approach that suppresses the undesired consumption of hydrogen peroxide, in particular, fractional addition of H_2O_2 , this decreases the amount of hydrogen peroxide spent for decomposition. This approach is known from the literature [52] and has been successfully used in our previous work [53–55]. Another way to reduce the hydrogen peroxide spent is the acidity regulation of reaction medium using Brønsted acidic centers [56].

Acid centers play an important role in the activation of both sulfides and peroxide. Authors [57] suggest that H_2O_2 could be electrophilically activated toward nucleophilic substrates with a Brønsted acid site. On the other hand, Brønsted acid sites on the surface of a support (for example, zeolite) or in an ionic liquid may contribute to the adsorption of sulfide [44,58–60]. The authors [59] showed that double activation is possible during the adsorption and transformation of thiophene on zeolites - the interaction of a proton (Brønsted acid site) with a sulfur atom and the cracking of thiophene catalyzed by Lewis basic oxygen atoms. Dual-activation model for the oxidation of thiophene on catalyst containing Brønsted IL and ammonium tungstate was proposed in [44]: the aromaticity of thiophene is partially destroyed by the hydrogen bonding with IL which contributes to its interaction with peroxocomplexes. Thus, the presence of acid sites in the catalyst along with polyoxometallate promotes catalysis.

The proposed SILP systems are also polyfunctional and promising for use in ODS and our results confirm this. The most active catalyst based on phosphomolybdic acid provides a high conversion rate for thiophene, thioanisole, and dibenzothiophene (turn over frequency of

about 150–1200 h^{-1} per mole of HPA). This is significantly higher than the data in the literature for thiophene [49] and DBT [23], even taking into account the difference in the reaction temperature (333 and 373 K respectively). Recycling experiments have demonstrated the stability of the catalyst. Finally, another important benefit of the reported systems is the desulfurization of diesel fuel with a very high efficiency (residual amount of sulfur < 10 ppm) under mild conditions.

2. Experimental

2.1. Materials

1,4-Butanesultone (99%), 1-ethylimidazole (95%), thiophene (99%), thioanisole (99%), dibenzothiophene (99%), phosphomolybdic acid (99%), phosphotungstic acid (99%), hydrogen peroxide solution (50 wt. % in H_2O) were purchased from Sigma-Aldrich. All other used solvents were obtained from commercial sources and used as received or distilled and dried using standard procedures.

Supports: Perkat 97-0 is a high-purity, beadshaped (bead size 3–5 mm), amorphous silica gel BASF. Granular γ - Al_2O_3 (0.4–1 mm size) JSC "Katalizator", Russia.

2.2. Preparation of catalysts

2.2.1. Preparation of 4-(3'-ethylimidazolium)-butanesulfonate

To synthesize 4-(3'-ethylimidazolium)-butanesulfonate, a modified method was used as described in [61]. 1,4-Butanesultone (13.6 g; 0.1 mol) with 1-ethylimidazole (9.4 g; 0.1 mol) were mixed in acetonitrile. The system was purged with argon and refluxed under inert gas purge for 24 h. The obtained white precipitate was filtered, washed two times with acetone and dried in vacuum at 353 K (Scheme 1). NMR spectra (Supplementary Material) of the resulting ionic liquid is equal to the ones reported in the [61].

2.2.2. Protonation IL with $H_3PMo_{12}O_{40}$ or $H_3PW_{12}O_{40}$ and wet impregnation

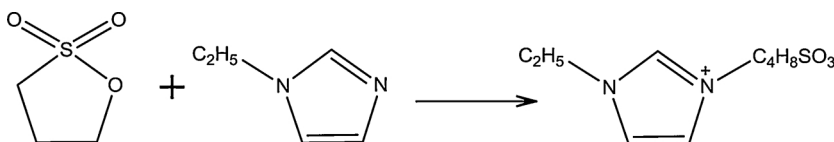
To obtain a protonated form, the sulfated ionic liquid was slowly added to an aqueous concentrated solution of the heteropolyacid ($H_3PMo_{12}O_{40}$ or $H_3PW_{12}O_{40}$). The mixture (IL to HPA in molar ratio of 3:1) was vigorously stirred for 6 h at room temperature and then the solvent was removed in air stream. The dried product was stored in busk.

All catalysts (Fig. 1) were prepared by wet impregnation of the support (γ - Al_2O_3 or Perkat) with an aqueous solution of protonated 4-(3'-ethylimidazolium)-butanesulfonate. For this the concentrated solution of the protonated IL was mixed with the support (mass ratio 1:10) at room temperature for 12 h. Then the solution was decanted and the resulting beads were washed twice with water. The obtained samples were dried for 2 h at 333–343 K in air stream.

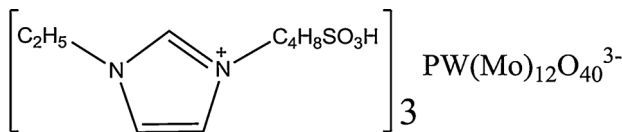
2.2.3. Catalyst characterization

The contents of molybdenum and tungsten on the catalyst surface were determined by photometry [62]. Electronic spectra were measured on a Shimadzu UV-2101PC.

The molecular composition and distribution over the catalyst surface for the compounds were determined by surface-assisted laser desorption/ionization (SALDI) mass spectrometry. The mass spectra were recorded in the RN Pep Mix mode on an Ultraflex Bruker instrument equipped with a nitrogen laser (337 nm wavelength, 110 μ J



Scheme 1. Synthesis of 4-(3'-ethylimidazolium)-butanesulfonate.



Support

Fig. 1. Structure of the synthesized catalysts.

energy) with a time-of-flight mass analyzer. The spectra were measured in the negative ion mode using a reflectron. The cluster ion identification based on isotopic distribution analysis was carried out using the IsoPro simulation program.

The acidic properties of the catalysts were studied by the temperature-programmed desorption of ammonia (NH_3 TPD) on a USGA-101 sorption analyzer (Unisit). The sample was annealed in a dry helium flow at 423 K and then cooled down to room temperature. The adsorption of ammonia (diluted with nitrogen in 1:1 ratio) was conducted for 30 min at 333 K. The physically sorbed ammonia was removed in a helium flow at 373 K for 1 h. The NH_3 TPD experiments were carried out in the temperature range of 333–873 K in a dry helium flow (flow rate of 30 mL/min). The heating rate was 281 K/min.

The catalyst surfaces were examined on a JEOL JSM – 6000 NeoScope scanning electron microscope with a built-in EX-230 energy dispersive X-ray analyzer. The images were recorded in a high vacuum at an accelerating voltage of 5 kV. The signal was detected in the secondary electron imaging (SEI) mode.

Adsorption measurements were carried out on an Micromeritics ASAP 20,000 N automated sorptometer. Prior to the measurements, the samples were evacuated at 473 K for 2 h.

2.2.4. Catalytic tests and analysis of the reaction products

The preparation of three model oils was carried out by dissolving of thiophene, thioanisole, and dibenzothiophene separately into three bottles that contained the required amounts of isoctane. The original substratum concentration of each model oil was around 1%.

All the oxidation experiments were conducted in the glass reactor (50 ml) equipped with a thermostatic jacket, a reflux condenser and magnetic stirrer (300 rpm mixing speed). The model oil (10 mL) and a catalyst (0.1 g) were added into the reactor at room temperature, and when the mixture was heated to 333 K, H_2O_2 (0.4 mL 50%) was added with stirring. For comparison, the activity of the pure supports was measured in the thiophene oxidation to the full stop.

The reaction was carried out for 0.5–4 h (0.5 h - time to reach maximum conversion of thioanisole, 4 h - dibenzothiophene). For fractional peroxide loading, H_2O_2 was loaded in batches by 0.2 mL every two hours. Samples were taken at intervals 0.5–1 h, and the organic phase was analyzed quantitatively by GC-FID with an internal standard. Kristall 2000 M chromatograph (Chromatec, Russia) was equipped with a capillary column (Zebtron ZB-1, 30 m \times 0.32 mm i.d. \times 0.5 μm). The products were identified by ^1H NMR on a Bruker Avance-600 instrument (600 MHz), $T = 298\text{ K}$ and by GC/MS analysis on a THERMO TRACE DSQ II instrument (Termo Fisher Sci.). To carry out the recycle experiment, a reaction solution was decanted and the catalyst was washed with isoctane.

For diesel desulfurization, the fuel (20 mL, S total content of 0.108% or 1080 ppm), a catalyst (0.04 g) and 0.4 mL H_2O_2 (50%) were stirred (300 rpm mixing speed) at 333 K for 4 h. Then, the solution was washed twice with DMF (5 mL) using a separation funnel. DMF was used for sulfur oxidation products extraction. This solvent exhibited more efficient extraction characteristics and the process is a necessary addition to the oxidation [28]. After this H_2O_2 (0.4 mL) was added to the washed solution and the mixture was stirred with the same catalyst, for another 4 h (fractional peroxide loading). For comparison, the process was carried out in one stage with H_2O_2 (0.8 mL). The sulfur content was

Table 1
Sample composition, textural characteristics, and acidity.

Samples	S^a ($\text{m}^2\text{ g}^{-1}$)	D_p^b (nm)	V_p^c (sm^3/g)	Mo or W (wt. %)	A ($\mu\text{mol NH}_3/\text{g}$)	ΔA^d ($\mu\text{mol NH}_3/\text{g}$)
$\gamma\text{-Al}_2\text{O}_3$	180	12	0.55	–	178	–
Perlkat 97-0 silica gel	300	10	0.75	–	20	–
PMoS/SiO ₂	114	9	0.33	1.6	231	211
PMoS/Al ₂ O ₃	120	11	0.36	0.9	301	123
PWS/SiO ₂	104	10	0.32	2.8	154	134
PWS/Al ₂ O ₃	108	11	0.28	1.2	218	40

Notes: a - BET surface area, b - D_p pore diameter (BJH), c - V_p pore volume (BJH), d - A(cat) – A(support).

determined on the X-ray fluorescence spectrometer ASE-2 (Limits of basic relative error $\pm 0.5\%$).

3. Results and discussion

3.1. Characterization of the catalyst

According to the IUPAC classification, the isotherms for all catalytic samples correspond to type IV, which is indicative of mesoporous surfaces [63]. A typical nitrogen adsorption isotherm is presented in Supplementary Material. The adsorption branches of all isotherms show a sharp inflection at a rather high relative pressure ($P/P_0 > 0.6$), which attests to typical capillary condensation in uniform pores. In turn, the hysteresis loops of all samples refer to H_1 type, which attests to a uniform distribution of agglomerates of active particles (this is in line with SEM data, Fig. 4) and a cylindrical pore geometry. Physicochemical parameters such as BET specific surface area and the pore size of the samples are summarized in Table 1. It can be seen from the Table that during the synthesis of all catalysts, the specific surface area and the pore volume obviously decrease. This decrease is in line with the metal content on the catalyst surface (Table 1). Apparently, the metal-containing IL fills small pores and mesopores located deep in the granules. Meanwhile, the average diameter of mesopores changes slightly, which implies that IL forms relatively thin layers (less than 0.5 nm) on the pore walls accessible to the adsorbate.

The acidic properties of the samples were characterized by NH_3 TPD. For comparison, to estimate the contribution of acidity of the protonated ionic liquid, NH_3 TPD experiments were carried out for the supports ($\gamma\text{-Al}_2\text{O}_3$ and Perlkat 97-0 silica gel) and for the PMoS/SiO₂, PMoS/Al₂O₃, PWS/SiO₂, and PWS/Al₂O₃ catalysts (Table 1). The samples are characterized by curves with maximum about 473 K (Supplementary Material). Analysis of the results summarized in the Table shows that the samples possess different numbers of acid sites. The total acidity of silica and alumina increases upon the formation of the IL layer on the surface, the contribution of the IL to the acidic properties being correlated with the IL content and being the highest for Mo derivatives.

According to the laser desorption/ionization data, the structure of ions on the surface depends on the type of the support. The mass spectra of phosphomolybdic (PMA) and phosphotungstic (PTA) heteropolyacids for comparison with the catalyst mass spectra were reported in [55]. It can be seen from the spectra in Figs. 2b and 3 b that during surface functionalization, heteropolyacid partly decomposes on alumina to give various polymolybdates and polytungstates: Mo_2O_7^- , Mo_3O_9^- , $\text{Mo}_4\text{O}_{12}^-$, $\text{Mo}_5\text{O}_{10}^-$, $\text{Mo}_6\text{O}_{12}^-$, W_2O_6^- , W_3O_9^- , $\text{W}_4\text{O}_{12}^-$, $\text{W}_5\text{O}_{15}^-$, $\text{W}_7\text{O}_{21}^-$, and $\text{W}_8\text{O}_{24}^-$. This result is consistent with the published information that during the synthesis of heterogeneous catalysts, the structure of phosphomolybdic and phosphotungstic acids on the alumina surface is deteriorated, because of the strong interaction between the heteropolyanions and the $\gamma\text{-Al}_2\text{O}_3$ surface [16,28,64,65].

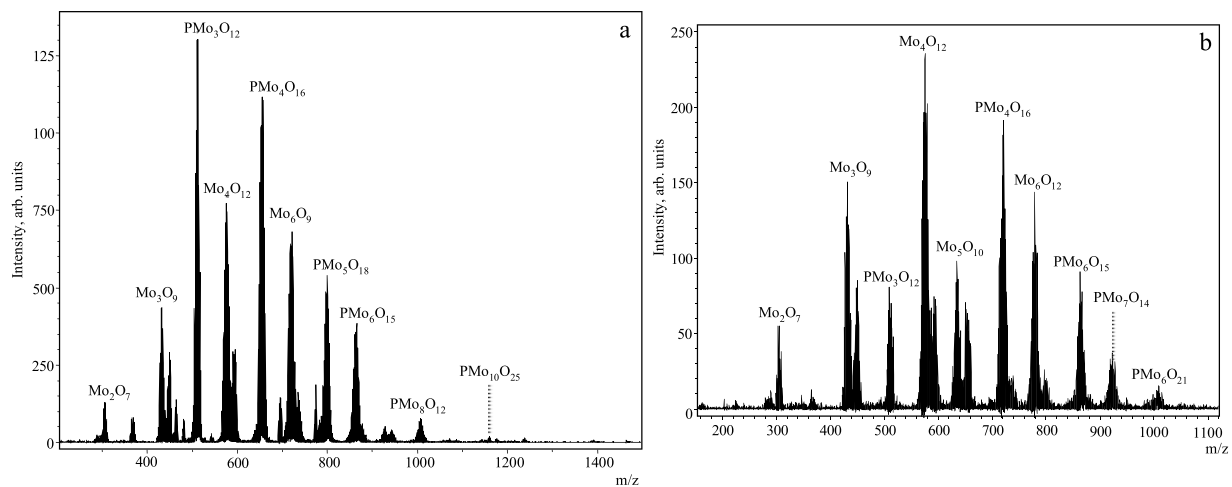


Fig. 2. SALDI mass spectra of PMoS/SiO₂ (a) and PMoS/Al₂O₃ (b) catalysts recorder in the negative ion direction mode.

Also, the mass spectra of samples exhibit peaks corresponding to the following heteropolyacid clusters: PMo₃O₁₂⁻, PMo₄O₁₆⁻, PMo₆O₁₅⁻, PMo₇O₁₄⁻, PMo₆O₂₁⁻, PW₃O₁₂⁻, and PW₆O₁₇⁻; a similar composition was found in the analysis of the starting HPA [55]. It is evident that the use of 4-(3'-ethylimidazolium)-butanesulfonate as a part of compositions contributes to stabilization of the heteropolyacid structure on the alumina surface. No deterioration of the PMA or PTA structure takes place on the Perlkat 97-0 silica gel surface. The spectra shown in Figs. 2a and 3a exhibit mainly the heteropolyanions: PMo₃O₁₂⁻, PMo₄O₁₆⁻, PMo₅O₁₈⁻, PMo₆O₁₅⁻, PMo₈O₁₂⁻, PMo₁₀O₂₅⁻, PW₂O₅⁻, PW₃O₁₂⁻, PW₄O₁₄⁻, PW₅O₁₅⁻, PW₆O₁₇⁻, and PW₁₂O₄₀⁻. The most intense peaks refer to the PMo₃O₁₂⁻ and PW₃O₁₂⁻ clusters, which attests to the stability of HPA during the synthesis of the PMoS/SiO₂ and PWS/SiO₂ catalysts.

The sample morphology was characterized by means of a SEM examination and presented in Supplementary Material. A comparison of the initial support surface with the surface of catalysts indicate that deposition of the protonated IL changes the support morphology slightly. The results of energy dispersive X-ray analysis of the surface sample (PMS/SiO₂) are presented in Fig. 4. According to the results, the IL was uniformly distributed on the outer surface of the Perlkat 97-0 silica gel. However, a decrease in the surface area and pore volume and size, especially SiO₂, indicated that the IL is also inside the support. In the case of Al₂O₃, the decreasing in surface area and pore volume were smaller due to the larger pore size of support. The decreasing in the average pore size by 1 nm indicated that IL fills the pore surface with a thin layer.

3.2. Catalytic properties of compositions

The catalytic properties of samples in the model thiophene oxidation conducted with one-shot or fractional addition of hydrogen peroxide are presented in Fig. 5. A comparison of sample activities demonstrated that molybdenum-containing compositions are more beneficial. This is in line with published data for PMA- and PTA-containing heterogeneous catalysts [66,67] and may be associated with high oxidative potential of phosphomolybdic acid [68]. The PMoS/SiO₂ sample proved to be the most active. This result can be attributed to high Mo content (Table 1) and enhanced stability of HPA on this support. Indeed, a relationship between the stability of heteropolyanions on the support surface and high catalyst activity is known from the literature [64]. Since in our study, the HPA structure is mainly retained upon the deposition of PMA on the Perlkat 97-0 silica gel and is partially destroyed in the case of γ-Al₂O₃ support, the highest catalytic activity is inherent in PMoS/SiO₂ (Fig. 5).

The highest activity of the PMoS/SiO₂ catalyst is correlated with its relative acidity ΔA (Table 1). Another sample (PMS/Al₂O₃) had even a higher total acidity, but a lower catalytic activity. This effect may be attributable to the interaction between the heteropolyanions and the γ-Al₂O₃ surface, which resulted in the partial decomposition of HPA (Fig. 3) and decreasing activity of the sample. In this case, the high acidity is caused not only by HPA (Brønsted) but also by Al₂O₃ (Lewis) acidity (Supplementary Material). It is known from the literature that the sample acidity has a beneficial effect on the catalytic activity towards the oxidation of sulfur compounds [45,69]. Apparently, the

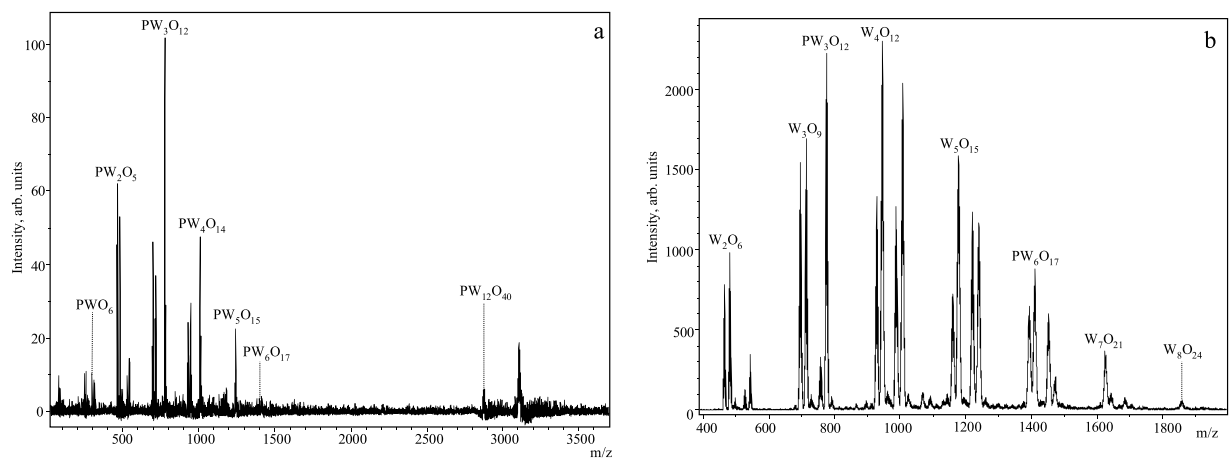


Fig. 3. SALDI mass spectra of PWS/SiO₂ (a) and PWS/Al₂O₃ (b) catalysts recorder in the negative ion direction mode.

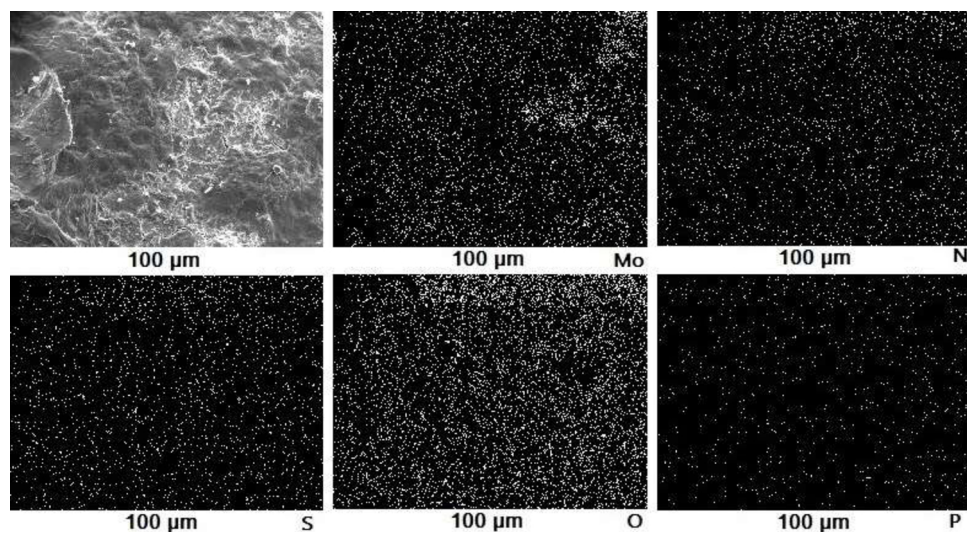


Fig. 4. The distribution of elements on the sample PMoS/SiO₂ surface.

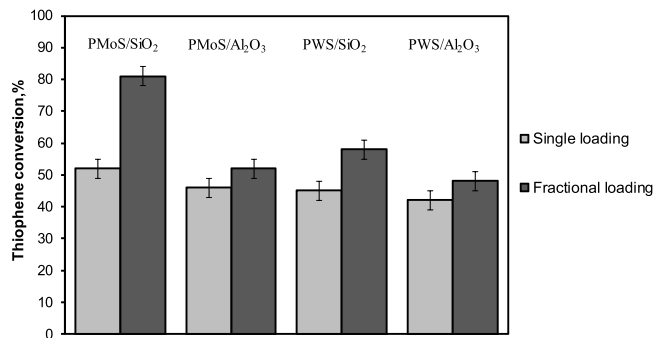


Fig. 5. Thiophene conversion upon one-shot and fractional addition of the oxidant. 4 h, 333 K, 0.4 mL of H₂O₂ (in the case of fractional addition, 0.2 mL every 2 h), 0.1 g of the catalyst.

acidic groups act as the adsorption sites for thiophene and its derivatives via the oxygen-sulfur interaction, which is also confirmed in the literature [70]. The addition of the acid to the reaction mixture is known to promote more extensive oxidation of sulfur compounds in homogeneous or two-phase systems [71,72]. However, the Al₂O₃ acidity was not enough for catalysis because the thiophene conversion on pure support during oxidation did not exceed 10% (6–8% on SiO₂). We suppose the Brønsted acid center in the cation to play the key role. In order to discriminate the effect of support (Brønsted and especially Lewis acidity), we considered the difference between the acidity of the sample and the support, which is especially important for Al₂O₃ (Table 1). The obtained values related to Bronsted acidity correlate with the activity of catalysts. In addition to this data, our assumption is consistent with [44]. As stated above, its authors proved that the hydrogen bonding between thiophene and acid cation distorted the planar structure and the aromaticity of thiophene. The synergistic effect of this

distortion with the catalytic oxidation function of heteropolyanion makes the thiophene activations more efficiently [44]. Thus, we believe (Fig. 6) the imidazolium cation immobilized on the surface adsorbs the substrate, the formation of a hydrogen bond between an acidic proton and a sulfur atom contributes to this process. Peroxocomplexes formed under the action of peroxide in the anionic part act on the thiophene molecule with a distorted aromatic structure. This double activation contributes to the catalytic reaction.

The effect of temperature on the thiophene oxidation rate is described by a function with an extremum. The dependence was studied in relation to the most active PMoS/SiO₂ catalyst in the temperature range of 313–353 K (Fig. 7). In the initial stage, a temperature rise is accompanied by the obvious increase in the catalyst activity up to a maximum (333–338 K), while further temperature rise decreases the process efficiency due to increasing rate of hydrogen peroxide decomposition. Thus, the effect of temperature follows a complex pattern, with the optimal temperature being in the narrow range (333–338 K). A similar dependence for catalytic systems containing heteropolyacids is described in our previous paper; therefore, all our research for sulfur compounds was carried out at the optimal temperature [55].

3.3. Catalysts in the oxidation of model substrates

According to the results of chemical and physicochemical analysis, sulfuric acid was formed as thiophene oxidation product, organic substances were not detected. It should be noted that published data on the composition of thiophene oxidation products are contradictory. The process may afford sulfoxide and sulfone, aldehydes, organic acids, styrene, sulfate anion, and carbon dioxide [51,72–74]. Analysis of published data suggests that the extensive oxidation that we observe involves destruction of the aromatic structure of thiophene to give the sulfate anion and carbon dioxide.

The high catalytic activity of the PMoS/SiO₂ sample accounts for

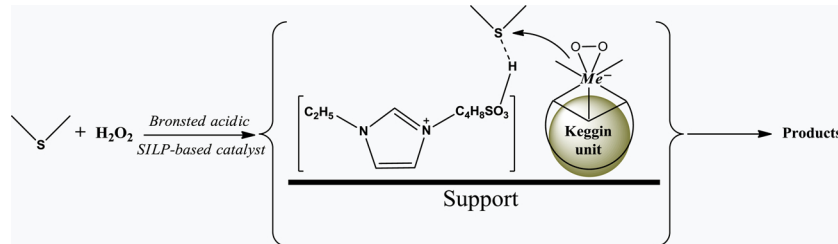


Fig. 6. Model for thiophene adsorption and oxidation on Brønsted SILP catalyst.

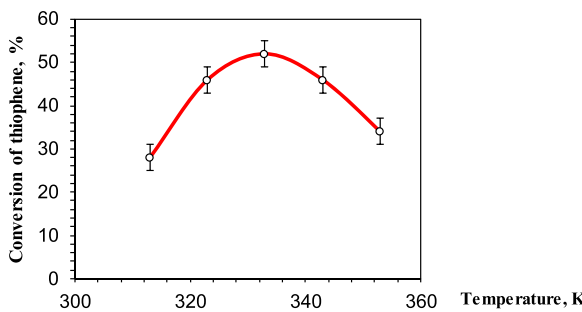


Fig. 7. Effect of temperature on the thiophene oxidation (313–353 K). Catalyst PMoS/SiO₂. 4 h, 0.1 g of the catalyst. One-shot addition of 0.4 mL of H₂O₂.

the side peroxide decomposition reaction. In order to decrease the undesirable consumption of the oxidant, fractional addition of hydrogen peroxide was used in the study. This method is known from the literature [52] and was successfully used in our previous work [53–55]. According to [75,76] the reaction order of hydrogen peroxide decomposition catalyzed by transition metals varies from second to zero depending on H₂O₂ initial concentration. The order of the main reaction remains unchanged – about first. Thus, the addition of the peroxide in small portions reduces the H₂O₂ concentration, due to the order increasing the decomposition reaction is slowed down and the ODS process becomes more efficient. As can be seen in Fig. 5, this technique boosted the thiophene conversion, which reached 80% for the most active sample. As follows from analysis of Fig. 5, the effect of fractional addition of the oxidant is especially pronounced for SiO₂-supported catalysts: under these conditions, the efficiency of the process increases by 30–60%.

It is known that thiophene is the most difficult to oxidize organo-sulfur substrate due to low electron density of the sulfur atom [42,43]. However, apart from thiophene, crude oil contains considerable amounts of quite a few sulfides and thiophene derivatives. Therefore, the PMoS/SiO₂ catalyst possessing high activity towards thiophene was tested in the oxidation of thioanisole and dibenzothiophene. As can be seen in Fig. 8, thioanisole and dibenzothiophene were oxidized much faster and to higher conversions. Even in the case of one-shot addition of the oxidant, the conversion rates per mole of HPA were very high, with turn over frequency (TOF) amounting to 140 h⁻¹ for thiophene, 190 h⁻¹ for dibenzothiophene, and 1230 h⁻¹ for thioanisole in relation to one mole of HPA. It was found by chromatography that the corresponding sulfones are the major products of thioanisole and dibenzothiophene conversion. The catalyst activity towards sulfur substrates decreases in the series: thiophene < dibenzothiophene < thioanisole. The pattern of this dependence is known from the literature [42,43]. It is also noteworthy that in the case of fractional addition of hydrogen peroxide, the PMoS/SiO₂ catalyst remains stable throughout five operation cycles, with the dibenzothiophene and thioanisole conversion reaching 100% (Fig. 9).

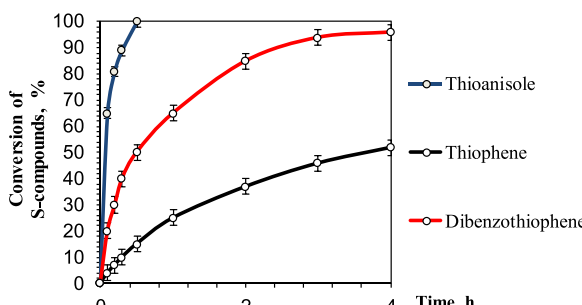


Fig. 8. Kinetic curves for the conversion of sulfur-containing substrates (thiophene, thioanisole, and dibenzothiophene). Catalyst PMoS/SiO₂. 4 h, 333 K, 0.1 g of the catalyst. One-shot addition of 0.4 mL of H₂O₂.

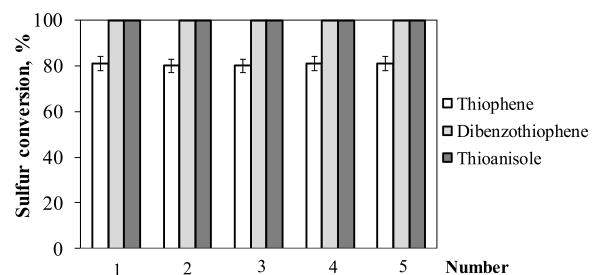


Fig. 9. Stability of the PMoS/SiO₂ catalyst in the oxidation of various substrates (thiophene, thioanisole, and dibenzothiophene) upon fractional addition of hydrogen peroxide. 4 h, 333 K, 0.1 g of the catalyst.

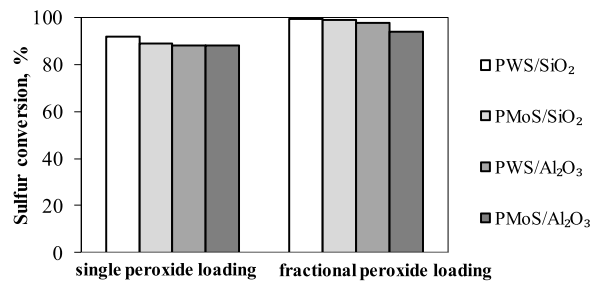


Fig. 10. Desulfurization of fuel: single loading (0.8 mL H₂O₂, 4 h) and fractional loading (0.4 mL + 0.4 mL H₂O₂ in 4 h) processes, 0.04 g of catalyst, 333 K, 20 mL of diesel fuel.

3.4. Catalysts in diesel oxidation

The results of diesel desulfurization were presented in Fig. 10. In this case, the most active catalyst was based on Phosphotungstic acid in contrast to model substrates. The best support material was SiO₂. All catalysts showed good results with fractional loading of hydrogen peroxide in two-stage purification of fuel. However, only two of them allowed obtaining the fuel that meets modern environmental requirements.

4. Conclusion

Thus, a method is proposed for the synthesis of heterogeneous catalysts based on sulfated IL (4-(3'-ethylimidazolium)-butanesulfonate) protonated by Mo- and W-based heteropolyacids. The nature of the support (γ -Al₂O₃ and Perlkat 97-0 silica gel) was found to influence the catalyst activity towards the thiophene oxidation. The most active catalyst was obtained from phosphomolybdic acid and was successfully tested in the oxidation of dibenzothiophene and thioanisole. The turnover frequency (TOF) per mole of HPA was 140 h⁻¹ for thiophene, 190 h⁻¹ for dibenzothiophene, and 1230 h⁻¹ for thioanisole. The fractional addition of the oxidant boosted the degree of oxidation for each of the tested substrates (thiophene, dibenzothiophene, thioanisole) by 20–50%. When using a catalyst PWS/SiO₂, a diesel fuel with residual sulfur content of 4 ppm was obtained.

Conflicts of interest

None.

Acknowledgement

This work was supported under the Moscow State University Development Program.

Appendix A. Supplementary data

Supplementary material related to this article can be found, in the online version, at doi:<https://doi.org/10.1016/j.apcatb.2019.117938>.

References

- [1] Z. Ismagilov, S. Yashnik, M. Kerzhentsev, V. Parmon, A. Bourane, F.M. Al-Shahrani, A.A. Hajji, O.R. Koseoglu, *Catal. Rev.* 53 (2011) 199–255.
- [2] M. Rezakzemi, Z. Zhang, *Compr. Energy Syst.* Elsevier, 2018, pp. 944–979.
- [3] V. Chandra Srivastava, *RSC Adv.* 2 (2012) 759–783.
- [4] R. Javadli, A. de Klerk, *Appl. Petrochem. Res.* 1 (2012) 3–19.
- [5] J.G. Speight, N.S. El-Gendy, *Introd. to Pet. Biotechnol.* Elsevier, 2018, pp. 165–227.
- [6] G. Mohebali, A.S. Ball, *Int. Biodeterior. Biodegrad.* 110 (2016) 163–180.
- [7] R. Dehghan, M. Anbia, *Fuel Process. Technol.* 167 (2017) 99–116.
- [8] A.M. Moreira, H.L. Brandão, F.V. Hackbarth, D. Maass, A.A. Ulson de Souza, S.M.A. Guelli U. de Souza, *Chem. Eng. Sci.* 172 (2017) 23–31.
- [9] J. Gao, S. Zhu, Y. Dai, C. Xiong, C. Li, W. Yang, X. Jiang, *Fuel* 233 (2018) 704–713.
- [10] W. Jiang, L. Dong, W. Liu, T. Guo, H. Li, S. Yin, W. Zhu, H. Li, *Chem. Eng. Process. Process. Intensif.* 115 (2017) 34–38.
- [11] K. Zhao, Y. Cheng, H. Liu, C. Yang, L. Qiu, G. Zeng, H. He, *RSC Adv.* 5 (2015) 66013–66023.
- [12] J.F. Palomeque-Santiago, R. López-Medina, R. Oviedo-Roa, J. Navarrete-Bolaños, R. Mora-Vallejo, J.A. Montoya-de la Fuente, J.M. Martínez-Magadán, *Appl. Catal. B: Environ.* 236 (2018) 326–337.
- [13] F. Mirante, L. Dias, M. Silva, S.O. Ribeiro, M.C. Corvo, B. de Castro, C.M. Granadeiro, S.S. Balula, *Catal. Commun.* 104 (2018) 1–8.
- [14] W. Abdul-Kadhim, M.A. Deraman, S.B. Abdullah, S.N. Tajuddin, M.M. Yusoff, Y.H. Taufiq-Yap, M.H.A. Rahim, *J. Environ. Chem. Eng.* 5 (2017) 1645–1656.
- [15] Y. Zhang, G. Li, L. Kong, H. Lu, *Fuel* 219 (2018) 103–110.
- [16] J.L. García-Gutiérrez, G.A. Fuentes, M.E. Hernández-Terán, F. Murrieta, J. Navarrete, F. Jiménez-Cruz, *Appl. Catal. A: Gen.* 305 (2006) 15–20.
- [17] M.A. Rezvani, M. Oveisí, M.A. Nia Asli, *J. Mol. Catal. A: Chem.* 410 (2015) 121–132.
- [18] G. Miao, D. Huang, X. Ren, X. Li, Z. Li, J. Xiao, *Appl. Catal. B: Environ.* 192 (2016) 72–79.
- [19] X. Zhou, C. Zhao, J. Yang, S. Zhang, *Energy Fuels* 21 (2007) 7–10.
- [20] H. Lü, J. Gao, Z. Jiang, Y. Yang, B. Song, C. Li, *Chem. Commun.* (2007) 150–152.
- [21] X. Zhou, J. Li, X. Wang, K. Jin, W. Ma, *Fuel Process. Technol.* 90 (2009) 317–323.
- [22] C. Ma, B. Dai, P. Liu, N. Zhou, A. Shi, L. Ban, H. Chen, *J. Ind. Eng. Chem.* 20 (2014) 2769–2774.
- [23] L. Kang, H. Liu, H. He, C. Yang, *Fuel* 234 (2018) 1229–1237.
- [24] L. Qiu, Y. Cheng, C. Yang, G. Zeng, Z. Long, S. Wei, K. Zhao, L. Luo, *RSC Adv.* 6 (2016) 17036–17045.
- [25] C. Yang, K. Zhao, Y. Cheng, G. Zeng, M. Zhang, J. Shao, L. Lu, *Sep. Purif. Technol.* 163 (2016) 153–161.
- [26] A. Bazyari, A.A. Khodadadi, A. Haghigat Mamaghani, J. Beheshtian, L.T. Thompson, Y. Mortazavi, *Appl. Catal. B: Environ.* 180 (2016) 65–77.
- [27] D. Wang, E.W. Qian, H. Amano, K. Okata, A. Ishihara, T. Kabe, *Appl. Catal. A: Gen.* 253 (2003) 91–99.
- [28] J.L. García-Gutiérrez, G.A. Fuentes, M.E. Hernández-Terán, P. García, F. Murrieta-Guevara, F. Jiménez-Cruz, *Appl. Catal. A: Gen.* 334 (2008) 366–373.
- [29] X. Shi, X. Han, W. Ma, J. Wei, J. Li, Q. Zhang, Z. Chen, *J. Mol. Catal. A: Chem.* 341 (2011) 57–62.
- [30] J.M. Ramos, J.A. Wang, L.F. Chen, U. Arellano, S.P. Ramírez, R. Sotelo, P. Schachat, *Catal. Commun.* 72 (2015) 57–62.
- [31] S. Wei, H. He, Y. Cheng, C. Yang, G. Zeng, L. Kang, H. Qian, C. Zhu, *Fuel* 200 (2017) 11–21.
- [32] M.A. Safa, X. Ma, *Fuel* 171 (2016) 238–246.
- [33] M.H. Ibrahim, M. Hayyan, M.A. Hashim, A. Hayyan, *Renew. Sustain. Energy Rev.* 76 (2017) 1534–1549.
- [34] R.L. Vekariya, *J. Mol. Liq.* 227 (2017) 44–60.
- [35] G.M.J. Al Kaisy, M.I. Abdul Mutualib, M.A. Bustam, J.-M. Leveque, N. Muhammad, *J. Environ. Chem. Eng.* 4 (2016) 4786–4793.
- [36] M. Safa, B. Mokhtarani, H.R. Mortaheb, *Chem. Eng. Res. Des.* 111 (2016) 323–331.
- [37] J. Wang, L. Zhang, Y. Sun, B. Jiang, Y. Chen, X. Gao, H. Yang, *Fuel Process. Technol.* 177 (2018) 81–88.
- [38] S. Gao, J. Li, X. Chen, A.A. Abdeltawab, S.M. Yakout, G. Yu, *Fuel* 224 (2018) 545–551.
- [39] N.L. Mai, K. Ahn, Y.-M. Koo, *Process Biochem.* 49 (2014) 872–881.
- [40] X. Zhang, D. Su, L. Xiao, W. Wu, *J. CO2 Util.* 17 (2017) 37–42.
- [41] Y. Wang, D. Zhao, L. Wang, X. Wang, L. Li, Z. Xing, N. Ji, S. Liu, H. Ding, *Fuel* 216 (2018) 364–370.
- [42] S. Otsuki, T. Nonaka, N. Takashima, W. Qian, A. Ishihara, T. Imai, T. Kabe, *Energy Fuels* 14 (2000) 1232–1239.
- [43] M. Li, M. Zhang, A. Wei, W. Zhu, S. Xun, Y. Li, H. Li, H. Li, *J. Mol. Catal. A: Chem.* 406 (2015) 23–30.
- [44] B. Zhang, Z. Jiang, J. Li, Y. Zhang, F. Lin, Y. Liu, C. Li, *J. Catal.* 287 (2012) 5–12.
- [45] H. Yang, B. Jiang, Y. Sun, L. Hao, Z. Huang, L. Zhang, *Chem. Eng. J.* 306 (2016) 131–138.
- [46] R. Skoda-Földes, *Molecules* 19 (2014) 8840–8884.
- [47] C. Song, *Catal. Today* 86 (2003) 211–263.
- [48] F.C.-Y. Wang, W.K. Robbins, F.P. Di Sanzo, F.C. McElroy, *J. Chromatogr. Sci.* 41 (2003) 519–523.
- [49] B. Zhang, Z. Jiang, J. Li, Y. Zhang, F. Lin, Y. Liu, C. Li, *J. Catal.* 287 (2012) 5–12.
- [50] K.N. Brown, J.H. Espenson, *Inorg. Chem.* 35 (1996) 7211–7216.
- [51] L. Kong, G. Li, X. Wang, *Catal. Lett.* 92 (2004) 163–167.
- [52] Y.L. Bi, M.J. Zhou, H.Y. Hu, C.P. Wei, W.X. Li, K.J. Zhen, *React. Kinet. Catal. Lett.* 72 (2001) 73–82.
- [53] I.G. Tarkhanova, A.A. Bryzhin, M.G. Gantman, T.P. Yarovaya, I.V. Lukiyanchuk, P.M. Nedozorov, V.S. Rudnev, *Surf. Coat. Technol.* 362 (2019) 132–140.
- [54] V.S. Rudnev, I.V. Lukiyanchuk, M.S. Vasilyeva, V.P. Morozova, V.M. Zelikman, I.G. Tarkhanova, *Appl. Surf. Sci.* 422 (2017) 1007–1014.
- [55] I.G. Tarkhanova, A.V. Anisimov, A.K. Buryak, A.A. Bryzhin, A.G. Ali-Zade, A.V. Akopyan, V.M. Zelikman, *Pet. Chem.* 57 (2017) 859–867.
- [56] H.S. Oh, J.-J. Kim, Y.-H. Kim, *Korean J. Chem. Eng.* 33 (2016) 885–892.
- [57] S. Liao, I. Čorić, Q. Wang, B. List, *J. Am. Chem. Soc.* 134 (2012) 10765–10768.
- [58] M.H.F. Kox, K. Domke, J.P.R. Day, G. Rago, E. Stavitski, M. Bonn, B. Weckhuysen, *Angew. Chem. Int. Ed.* 48 (2009) 8990–8994.
- [59] X. Rozanska, R.A. van Santen, F. Hutschka, *J. Catal.* 200 (2001) 79–90.
- [60] S.Y. Yu, J. Garcia-Martinez, W. Li, G.D. Meitzner, E. Iglesia, *Phys. Chem. Chem. Phys.* 4 (2002) 1241–1251.
- [61] Q. Wu, W. Li, M. Wang, Y. Hao, T. Chu, J. Shang, H. Li, Y. Zhao, Q. Jiao, *RSC Adv.* 5 (2015) 57968–57974.
- [62] W.T. Elwell, D.F. Wood, *Int. Ser. Monogr. Anal. Chem.* Elsevier, 1971, pp. 15–21.
- [63] R. Haul, *Berichte Der Bunsengesellschaft Für Phys. Chem.* 86 (1982) 957–957.
- [64] M. Sopa, A. Waclaw-Held, M. Grossy, J. Pijanka, K. Nowińska, *Appl. Catal. A: Gen.* 285 (2005) 119–125.
- [65] G. Marci, E. García-López, M. Bellardita, F. Parisi, C. Colbeau-Justin, S. Sorgues, L.F. Liotta, L. Palmisano, *Phys. Chem. Chem. Phys.* 15 (2013) 13329–13342.
- [66] M. Craven, D. Xiao, C. Kunstmann-Olsen, E.F. Kozhevnikova, F. Blanc, A. Steiner, I.V. Kozhevnikov, *Appl. Catal. B: Environ.* 231 (2018) 82–91.
- [67] E. Rafiee, N. Nobakht, *J. Mol. Catal. A: Chem.* 398 (2015) 17–25.
- [68] I.V. Kozhevnikov, *Chem. Rev.* 98 (1998) 171–198.
- [69] X. Chen, D. Song, C. Asumana, G. Yu, J. Mol. Catal. A: Chem. 359 (2012) 8–13.
- [70] A.R. Lopes, A. de P. Scheer, G.V. Silva, C.I. Yamamoto, *Matéria (Rio Janeiro)* 21 (2016) 407–415.
- [71] F. Al-Shahrani, T. Xiao, S.A. Llewellyn, S. Barri, Z. Jiang, H. Shi, G. Martinie, M.L.H. Green, *Appl. Catal. B: Environ.* 73 (2007) 311–316.
- [72] L. Chen, S. Guo, D. Zhao, *Chin. J. Chem. Eng.* 15 (2007) 520–523.
- [73] R.M. Mohamed, E.S. Aazam, *Appl. Catal. A: Gen.* 480 (2014) 100–107.
- [74] C. Yang, H. Ji, C. Chen, W. Ma, J. Zhao, *Appl. Catal. B: Environ.* 235 (2018) 207–213.
- [75] L. Kreja, A. Plewka, *Angew. Makromol. Chem.* 102 (1982) 45–58.
- [76] L. Kreja, *Mon. Chem.* 118 (6–7) (1987) 717–726.